

Pinning/depinning of crack fronts in heterogeneous materials

P. Daguier[†], B. Nghiem[‡], E. Bouchaud[†] and F. Creuzet[‡]

[†]*O.N.E.R.A. (OM), 29 Avenue de la Division Leclerc,*

B.P. 72, 92322 Châtillon Cedex, FRANCE

[‡]*Laboratoire CNRS/Saint-Gobain “Surface du Verre et Interfaces”, 39, Quai Lucien Lefranc,*

B.P. 135, 93303 Aubervilliers Cedex, FRANCE

The fatigue fracture surfaces of a metallic alloy, and the stress corrosion fracture surfaces of glass are investigated as a function of crack velocity. It is shown that in both cases, there are two fracture regimes, which have a well defined self-affine signature. At high enough length scales, the universal roughness index $\zeta \simeq 0.78$ is recovered. At smaller length scales, the roughness exponent is close to $\zeta_c \simeq 0.50$. The crossover length ξ_c separating these two regimes strongly depends on the material, and exhibits a power-law decrease with the measured crack velocity $\xi_c \propto v^{-\phi}$, with $\phi \simeq 1$. The exponents ν and β characterising the dependence of ξ_c and v upon the pulling force are shown to be close to $\nu \simeq 2$ and $\beta \simeq 2$.

PACS numbers: 62.20.Mk, 05.40.+j, 81.40.Np

The pinning/depinning transition [1,2] has been the subject of many theoretical studies in the recent years [3]. But although there are in principle numerous applications, experimental examples remain scarce. In this letter, we analyse experimental results concerning crack propagation in two very different materials – a metallic alloy and glass – within the framework of models of pinning/depinning of moving lines through randomly distributed obstacles [4,5].

Fracture surfaces of many heterogeneous materials have been studied, with different experimental techniques. As shown first by Mandelbrot *et al* [6], these surfaces are self-affine [7], with a roughness index ζ in most cases close to the value 0.8. This quantity was later conjectured to be universal [8,9], i.e. independant of the material and of the fracture mode. As far as metallic materials are concerned, this exponent has been recently characterized over five decades of length scales (0.5 nm–0.5 mm) [10,11]. This universality was first questioned by Milman *et al* [12] on the basis of Scanning Tunneling Microscopy experiments where fracture surfaces of metallic materials were investigated at the nanometer scale. The reported values of roughness exponents in the latter case were significantly smaller than 0.8, closer to 0.5. This has been interpreted [10,13] as a kinetic effect similar to the one expected for a moving line near its depinning transition. Indeed, it was proposed recently that a fracture surface could be modelled as the *trace* left by the crack front moving through randomly distributed microstructural obstacles [14].

Various models have been developed to calculate the critical exponents characterising the morphology of these lines either in 2 dimensions (moving front) or in 3 dimensions (moving front leaving a surface behind it). Ertaş and Kardar studied a local nonlinear three-dimensional Langevin equation to describe the morphology of polymers in shear flows or the motion of flux lines in superconductors [4], and it was conjectured that these models

might also be relevant for fracture [14]. The line is pulled away with a constant force F . Non linearities account for the variations of the local crack speed with the local orientation of the front. This equation leads to a large number of regimes, depending on the relative values of the prefactors of the non linear terms. For some values, this model predicts that for a finite velocity v , the roughness exponent is 0.75 at “large length scales” and 0.5 at “short length scales”, the two regimes being separated by a crossover length ξ_c . The short length scales regime corresponds to the vicinity of the depinning transition [1,2] where the crack front is just able to free itself from the pinning microstructural obstacles. In this case, i.e. when F is close although higher than a critical force F_c under which the line remains still, the velocity v tends to zero, $v \propto (F - F_c)^\beta$, and ξ_c diverges as $\xi_c \propto v^{-\phi}$. In this particular model [4], $\phi = 3$. It will be shown in the following that the observed behavior is in qualitative agreement with this scenario [10], although the measured value of ϕ is significantly smaller.

Note that this behavior also corresponds to the results of recent large-scale molecular dynamics simulations [15–17] for amorphous materials.

In this letter, quantitative results are presented, which show that ξ_c indeed decreases with the crack velocity, and lead to an estimate of ϕ . Variations of the crossover length ξ_c with the average crack velocity are presented here both for the fatigue fracture of the Ti₃Al-based Supera₂ intermetallic alloy and for the stress corrosion fracture of soda-lime silica glass.

Two notched compact tension specimens of Supera₂ are broken in fatigue. Fatigue tests are carried out using an electro-servo-hydraulic testing machine, operating under load control. The test is performed in air with a constant stress ratio $R = \sigma_{min}/\sigma_{max} = 0.1$ (σ_{max} and σ_{min} are respectively the minimum and the maximum stresses), at a frequency $f = 30\text{Hz}$. The evolution of the crack length a with time is measured with the potential

drop method [18]. The fracture surfaces are observed for 4 different velocities spanning a wide range, using both an atomic force microscope (AFM) and a standard scanning electron microscope (SEM). The SEM observations consist in cutting and polishing the NiPd-plated fractured samples perpendicularly to the direction of crack propagation and registering images of the profiles at various magnifications for each of the 4 regions (see [19]). For AFM observations, five profiles of length $1\text{ }\mu\text{m}$ are registered in each region.

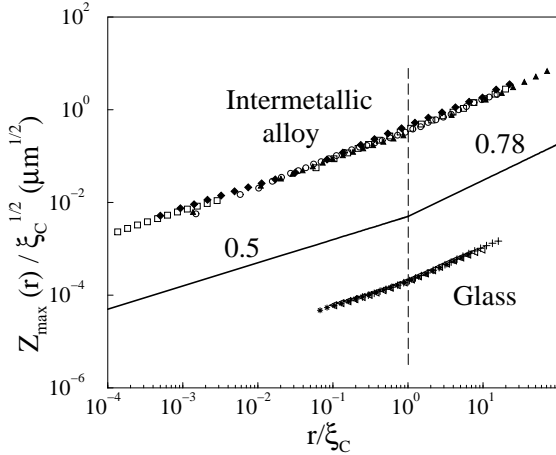


Fig 1: $Z_{max}(r)/\sqrt{\xi_c}$ is plotted against r/ξ_c for the two materials separately. Note that in these reduced units, the plots corresponding to the various velocities collapse on the same curve. Although the crossover regions are quite different for the two materials, the asymptotic regimes are well described by power laws with exponents 0.5 ($r/\xi_c \ll 1$) and 0.78 ($r/\xi_c \gg 1$).

Fracture surfaces of soda-lime silica glass have been prepared by controlling the crack propagation with a four points bending system. After the initial propagation, which allows to relax all residual stresses, the plate is properly loaded in order to obtain the required average crack velocity. This velocity is measured by imaging the crack tip with AFM at different times. The humidity rate has been measured, and kept between 37 and 41%. The controlled crack propagation is maintained over a distance of about $30\text{ }\mu\text{m}$, so that fracture surfaces can be easily probed with AFM. Crack velocities range from $2 \cdot 10^{-9}$ to 10^{-7} ms^{-1} . Ten AFM height profiles of length $1.5\text{ }\mu\text{m}$ are registered perpendicularly to the direction of crack propagation, on three samples, and along this direction for four other specimens. As it will be shown in the following, no significant anisotropy could be detected.

In order to determine the roughness exponents ζ and the crossover length ξ_c of the profiles recorded, the Hurst method is used [21], where the following quantity is computed: $Z_{max}(r) = \langle \max[z(r')]_{r_o < r' < r_o+r} - \min[z(r')]_{r_o < r' < r_o+r} \rangle_{r_o}$, $Z_{max}(r) \propto r^\zeta$. r is the width of

the window, and $Z_{max}(r)$ is the difference between the maximum and the minimum heights z within the window, averaged over all possible origins r_o of the window belonging to the profile.

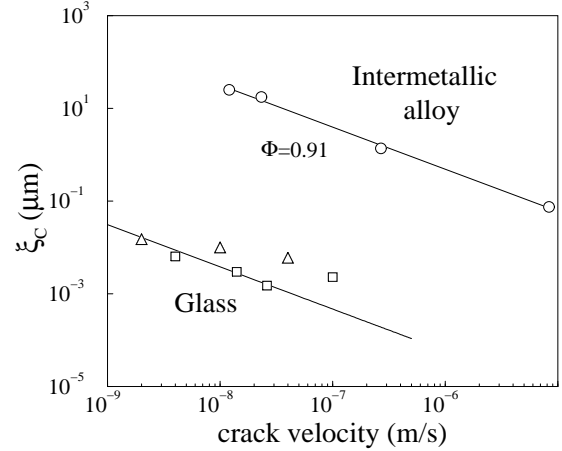


Fig 2: Evolution of the cross over length ξ_c with the crack velocity for the Super α_2 (o) and for soda-lime silica glass (Δ/\square : perpendicular/parallel to the direction of crack propagation). ξ_c is plotted versus v on a log-log plot, exhibiting a power-law dependence with an exponent $\phi \simeq 0.91$.

As far as the Super α_2 is concerned, the simultaneous use of SEM and AFM allows for an observation of the fracture surfaces over 5 or 6 decades of length scales. Within the whole range of observations, $Z_{max}(r)$ is very well fitted by the sum of two power laws, $Z_{max}(r) = A((r/\xi_c)^{0.5} + (r/\xi_c)^{0.78})$. The small and large length scales roughness indices -0.5 and 0.78 respectively, are chosen to fit with the results of previous experiments [10]. On the contrary, the crossover between the two regimes is much sharper in the case of glass (which seems to be the case for other amorphous materials [16,17]), and in this case, the crossover length ξ_c is determined as the intersection of the two asymptotic power law regimes with exponents 0.5 and 0.78. Once the crossover lengths have been determined in each case, it is possible to plot Z_{max} as a function of r/ξ_c . In Fig. 1, the curves $Z_{max}(r)/\sqrt{\xi_c}$ relative to each material are plotted as a function of r/ξ_c and shown to collapse on the same master curve. In both cases, the asymptotic regimes are well described by power laws with exponents 0.5 at small length scales ($r/\xi_c \ll 1$), and 0.78 at large length scales ($r/\xi_c \gg 1$). In other words, one can write:

$$Z_{max}(r) \propto r^{0.5} f\left(\frac{r}{\xi_c}\right) \quad (1)$$

with $f(x \rightarrow 0) \sim 1$ and $f(x \gg 1) \sim x^{0.28}$, showing that the amplitude of the small length scales contribution is independent of crack velocity.

The results obtained on materials as different as an

intermetallic alloy and a glass thus confirm previous observations [10,13], where the short and large length scales regimes were interpreted, respectively, as a “quasi-static” and a “dynamic” regime.

As it can be seen in Fig. 2, ξ_c decreases with the crack velocity v in both cases, although the measured values of ξ_c are approximately 1000 times larger in the case of the Super α_2 than in the case of glass. The experimental results are compatible with a power law decrease $v^{-\phi}$ in both cases. However, the estimated value of ϕ is close to unity instead of 3. Note that the values of ξ_c measured for glass for the higher velocities might be overestimated: in this case the precision is very bad, since ξ_c is of the order of some nanometers, i.e. close to the limit resolution of the AFM.

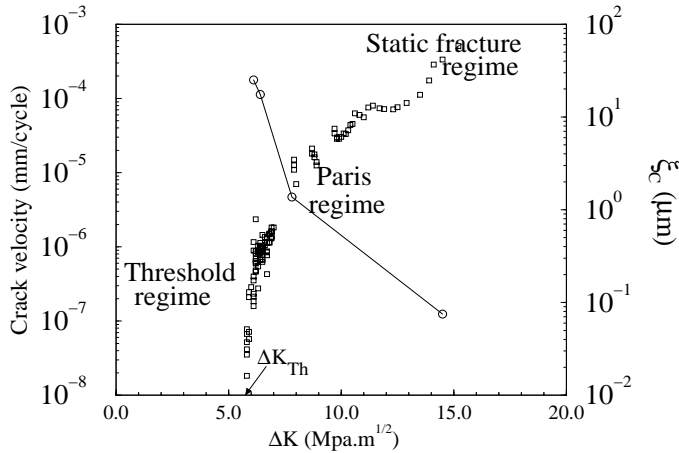


Fig 3: Super α_2 : the fatigue crack velocity (\square) as well as the cross over length ξ_c (\circ) are plotted against the stress intensity factor ΔK . The threshold value ΔK_{Th} is indicated.

In Fig. 3, both ξ_c and v are plotted against the stress intensity factor $\Delta K = (\sigma_{max} - \sigma_{min})\sqrt{a}$. The fatigue crack growth in this regime is widely known as intermittent [24,25]. In this regime, the crack tip opens and closes many times before it can extend over a small distance. This process is repeated several times and causes incremental crack advance. The number of cycles required to get the crack to advance decreases as ΔK increases, and the crack motion is more and more continuous, microstructural obstacles being efficient at smaller length scales. At a given time, the force F exerted on the fracture front is proportional to ΔK , while the threshold force F_c is proportional to ΔK_{Th} (defined in Fig. 3). The frequency of oscillation of these forces being far more rapid than crack propagation, the average force only can be considered, which legitimates the analogy with the above-quoted models. In the case of glass, F is proportional to the stress intensity factor K , while F_c is proportional to the threshold K_{Th} . Preliminary results indicate that, in the sub-critical regime, the crack veloc-

ity is not uniform, and intermittency is likely to occur. Thus, in both cases, the pinning/depinning scenario is qualitatively satisfactory.

Fig. 4 shows the evolution of the crack velocity v as a function of $\Delta K - \Delta K_{Th}$ for the Super α_2 and as a function of $K - K_{Th}$ for glass. In the case of the Super α_2 , experimental measurements reveal a power law increase without any change between the so-called “threshold” and Paris regimes. On the contrary, when static fracture occurs, a clear deviation from the power law can be observed for high values of $\Delta K - \Delta K_{Th}$. A fit of these data gives $\beta \simeq 2$. This value is compatible with the measurements on glass (Fig. 4).

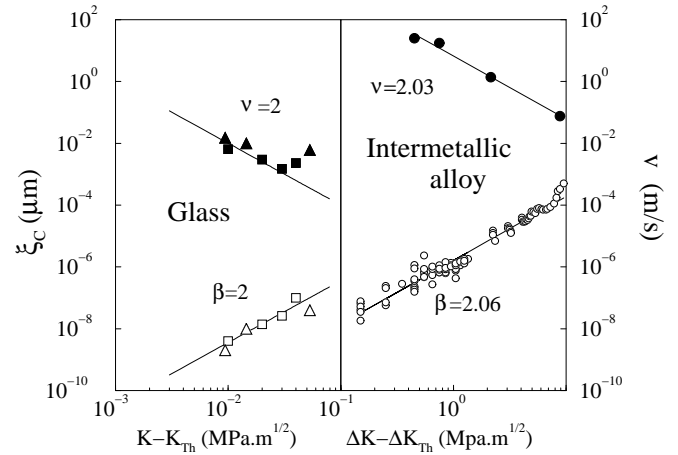


Fig 4: Super α_2 (\circ): the fatigue crack velocity (white symbols) is plotted versus $\Delta K - \Delta K_{Th}$ on a log-log plot, as well as the crossover length ξ_c (black symbols).

Glass (Δ/\square perpendicular/parallel to the direction of crack propagation): the crack velocity is plotted as a function of $K - K_{Th}$ (white symbols), as well as ξ_c (black symbols).

In Fig. 4, ξ_c is plotted also for both materials. A power law decrease can be observed, and the fit of the data relative to the metal gives $\nu \simeq 2$, compatible with the results on glass.

One can note that $\phi = \nu/\beta \simeq 1$. On the other hand, it is expected that the exponent n characterising the range of interactions ($n = 2$ for short range forces [1] and $n = 1$ for long range ones [5]) is related to the exponents ν and $\zeta_{||}$ through the relation:

$$n = \zeta_{||} + \frac{1}{\nu} \quad (2)$$

where $\zeta_{||}$ is the in-plane roughness exponent [26]. $\zeta_{||}$ was determined previously on the Super α_2 [26], and shown to be close to $\zeta_{||} \simeq 0.54$. This leads to a value of $n \simeq 1.03$ very close to unity, as expected for elastic interactions [5,22,23]. Note that the 2d model of Thomas

and Paczuski [23] leads to $\zeta = 0.5$ and $\nu = 2$, but also to $\beta = 1$.

Knowing β and ν , one can in principle deduce the value of the dynamic exponents z_{\parallel} and z_{\perp} describing the short time evolution of the front, respectively in the direction of crack propagation and perpendicularly to it. $z_{\parallel} = \zeta_{\parallel} + \frac{\beta}{\nu}$ leads to $z_{\parallel} \simeq 1.5$, while $z_{\perp} = z_{\parallel} + \frac{1}{\nu}$ should indicate that $z_{\perp} \simeq 2$. Hence, perturbations on the crack front are diffusive perpendicularly to the direction of crack propagation, while they are slightly hyper-diffusive along this direction.

For ductile materials as the Super α_2 , the plastic zone size R_{plast} should be a relevant length scale as well. Although the same behaviour is observed within the whole range of ΔK s, it can be noted that R_{plast} overpasses ξ_c for the two experiments corresponding to higher velocities.

The transition between the threshold regime and the Paris regime might be associated respectively with $\xi_c > R_{plast}$ and $\xi_c < R_{plast}$. It has been shown in Fig. 2 that a coarser microstructure gives rise to a higher ξ_c for the same crack velocity. On the other hand, Yoder *et al* [20] showed that, in the case of a titanium-based alloy, a coarser microstructure corresponds to a higher value of ΔK at which the transition occurs. This result supports the idea that the transition between the threshold regime and the Paris regime could be associated to a competition between R_{plast} and ξ_c . Note also that in the case of glass, the plastic zone size has been estimated [27] to be of the order of some nanometers, i.e. of the order of magnitude of ξ_c .

Further experiments on different materials are needed in order to confirm the general character of the pinning/depinning scenario, and to allow for a more precise determination of the critical exponents. In order to investigate the role of plasticity, experiments will be performed on an aluminium alloy, for which plastic zones are much larger than in the case of the Super α_2 .

Acknowledgements: The authors are particularly indebted to S. Navéos and G. Marcon for their technical help, and to J.-P. Bouchaud, E. Orignac and S. Roux for enlightening discussions.

[1] O. Narayan, D. Fisher, Phys. Rev. Lett. **68**, 3615 (1992); Phys. Rev. B **46**, 11520 (1992); O. Narayan, D. S. Fisher, Phys. Rev. B **48**, 7030 (1993).
[2] T. Nattermann, S. Stepanow, L.-H. Tang, H. Leschhorn, J. Phys. II (France) **2**, 1483 (1992).

[3] T. Halpin-Healy, Yi-Cheng Zhang, Physics Report, **254**, 215 (1995), and references therein.
[4] D. Ertas, M. Kardar Phys. Rev. Lett. **69**, 929 (1992); D. Ertas, M. Kardar Phys. Rev. E **48** 1228 (1993).
[5] D. Ertas, M. Kardar Phys. Rev. Lett. **73**, 1703 (1994); D. Ertas, M. Kardar, Phys. Rev. B **53**, 3520 (1996).
[6] B.B. Mandelbrot, D.E. Passoja, A.J. Paullay, Nature **308** 721 (1984).
[7] B.B. Mandelbrot, Phys. Scr. **32**, 257 (1985).
[8] E. Bouchaud, G. Lapasset, J. Planès, Europhys. Lett. **13**, 73 (1990).
[9] K.J. Maloy, A. Hansen, E. L. Hinrichsen, S. Roux, Phys. Rev. Lett. **68**, 213 (1992).
[10] P. Daguiet, S. Hénaux, E. Bouchaud and F. Creuzet, Phys. Rev. E **53**, 5637 (1996).
[11] P. Daguiet, E. Bouchaud in *Fracture-Instability Dynamics, Scaling, and Ductile/Brittle Behavior*, MRS Fall Meeting December 1995, **409**, Edited by R. L. Blumberg-Selinger, J. J. Mecholsky, A. E. Carlsson, E. R. Fuller, p. 343 (1996).
[12] V.Y. Milman, R. Blumenfeld, N.A. Stelmashenko, R.C. Ball, Phys. Rev. Lett. **71**, 204 (1993); V.Y. Milman, N.A. Stelmashenko, R. Blumenfeld, Prog. Mater. Sci. **38**, 425 (1994).
[13] E. Bouchaud, S. Navéos, J. Phys. I France **5**, 547 (1995).
[14] J.-P. Bouchaud, E. Bouchaud, G. Lapasset, J. Planès, Phys. Rev. Lett., **71**, 2240, (1993) ; E. Bouchaud, J.-P. Bouchaud, J. Planès, G. Lapasset, Fractals, **1**, 1051, (1993).
[15] A. Nakano, R. K. Kalia, P. Vashishta, Phys. Rev. Lett. **73**, 2336 (1994).
[16] A. Nakano, R. K. Kalia, P. Vashishta, Phys. Rev. Lett. **75**, 3138 (1995).
[17] R. K. Kalia, A. Nakano, A. Omeltchenko, K. Tsuruta, P. Vashishta, preprint (1996).
[18] R.O. Ritchie, K. J. Bathe, Int. J. of Fracture **15**, 47 (1979).
[19] E. Bouchaud in *Size-scale effects in the failure mechanisms of materials and structures*, IUTAM Symposium Turin October 1994, Edited by A. Carpinteri, E&F Spon (London), p. 121 (1996).
[20] G.R. Yoder, L.A. Cooley and T.W. Crooker, Eng. Fract. Mech., **11**, 805 (1979).
[21] J. Schmittbuhl, J.P. Vilotte, S. Roux, Phys. Rev. E **51**, 131 (1995).
[22] J. Schmittbuhl, S. Roux, J.-P. Vilotte, K. J. Maloy, Phys. Rev. Lett. **74**, 1787 (1995).
[23] P. B. Thomas, M. Paczuski, preprint (1996).
[24] J. Lankford and D.L. Davidson, Acta Metall. **31**, 1273 (1983).
[25] C. Bathias and J.P. Bailon, *La fatigue des matériaux et des structures*, Ed. Maloine S.A. (1980).
[26] P. Daguiet, E. Bouchaud, G. Lapasset, Europhys. Lett. **31**, 367 (1995).
[27] E. Guilloteau, H. Charrue, F. Creuzet, Europhys. Lett. **34**, 549 (1996).